

G-CSF treatment of canine cyclical neutropenia: A comprehensive mathematical model

Caroline Colijn^a, Catherine Foley^a, and Michael C. Mackey^{a,b,c}

^aDepartments of Mathematics; ^bPhysiology; ^cPhysics, Center for Nonlinear Dynamics in Physiology and Medicine, McGill University, Montreal, QC, Canada

(Received 16 November 2006; revised 20 February 2007; accepted 27 February 2007)

Objective. To study the effects of different G-CSF temporal treatment schemes using a comprehensive mathematical model of the mammalian hematopoietic system that couples the pharmacokinetics of granulocyte colony-stimulating factor (G-CSF) to the hematopoietic stem cell, neutrophil, platelet, and erythrocyte dynamics.

Materials and Methods. Data from cyclical neutropenic (CN) grey collies are used to build an extended model that reproduces the dynamics of circulating blood cells found in laboratory data from the dogs with and without daily G-CSF therapy. The effects of varying the treatment initiation time, and whether injections are given daily, every other day, or every three days, are examined.

Results. The mathematical model is able to reproduce the large variation in data that occurs from one dog to another. Different drug delivery times, with no other changes in the model parameters, can have significant long-term effects on neutrophil numbers. The frequency of drug delivery also has long-term effects on the oscillations.

Conclusion. Using a realistic representation of the effects of G-CSF on the tissue-level hematopoietic system, the model matches a wide range of laboratory data. This implies that it would be possible to generate individualized predictions for specific dogs if data were available in real time. The proposed interventions are practical and may reduce the amount of G-CSF required while potentially maintaining or even improving the treatment effects. © 2007 International Society for Experimental Hematology. Published by Elsevier Inc.

All blood cells are derived from the hematopoietic stem cells (HSC), which are undifferentiated cells having a high proliferative potential. These multipotent stem cells can proliferate and mature to form all types of blood cells (platelets, leukocytes, and erythrocytes). Production in these cell lineages is regulated by a variety of cytokines, including erythropoietin (EPO), which mediates the regulation of erythrocyte production, thrombopoietin (TPO), which regulates production of platelets (but may also affect other cell lineages), and granulocyte colony-stimulating factor (G-CSF), which regulates neutrophil numbers.

In Colijn and Mackey [1,2] a comprehensive mathematical model for the regulation of hematopoiesis was presented. This work was motivated by the existence of several hematological diseases that display a highly dy-

namic nature characterized by oscillations in one or more of the circulating cell lineages [3]. Examples of these are cyclical neutropenia, periodic chronic myelogenous leukemia, cyclical thrombocytopenia, and periodic hemolytic anemia.

In this paper, we concentrate on cyclical neutropenia, a rare hematological disorder characterized by oscillations in the circulating neutrophil count. Neutrophil levels fall from normal to barely detectable levels with a typical period of 19 to 21 days in humans [3–5], although periods up to 40 days have been observed [3]. These oscillations in the neutrophil count are generally accompanied by oscillations with similar period in the platelets, lymphocytes, and reticulocytes [3,6]. Cyclical neutropenia also occurs in grey collies with periods on the order of 11 to 16 days [3,6,7]. This animal model has provided extensive experimental data that has enriched our understanding of cyclical neutropenia. Though the gene modification responsible for canine cyclical neutropenia has been identified [8], the dynamic origin of the cycling is only partially understood.

Offprint requests to: Catherine Foley, M.Sc., Dept. of Mathematics, Center for Nonlinear Dynamics in Physiology and Medicine, McGill University, 3655 Promenade Sir William Osler, Montreal, Quebec, Canada H3G 1Y6; E-mail: foley@math.mcgill.ca

Because of its interesting dynamical nature, many mathematical models have been formulated to attempt to answer this question. While many have modeled cyclical neutropenia as arising only from destabilization of neutrophil dynamics [9,10], the work of Bernard et al. [11] and Colijn and Mackey [1] suggest that the origin of cyclical neutropenia lies in a destabilization of the combined HSC and neutrophil control system. The hypothesis that oscillations originate in the stem cells is supported by the observation that in cyclical neutropenia oscillations are also present in platelets and reticulocytes. Cyclical neutropenia in humans is often treated using G-CSF [12], which is known to interfere with apoptosis [13–16]. Treatment protocols typically call for daily subcutaneous injection of G-CSF at 3 to 5 μg per kg of body weight [17,18]. This represents a current cost of over US\$45,000 per year for a 70-kg adult. Clearly it would be of enormous economic benefit if the same clinical effects could be achieved with less G-CSF. A few alternative treatment strategies in humans have been reported in which various administration schemes have been used; for example, Jayabose and Sandoval [19] reported that three G-CSF doses weekly was clinically effective as well as cost effective.

In Bernard et al. [11], a two-compartment model accounting for a destabilization of the HSC compartment was used to mimic the dynamical behavior of the hematopoietic system under G-CSF treatment. In Foley et al. [20] the authors showed that, depending on the starting date of the G-CSF treatment, the neutrophil count could either be stabilized or show large amplitude oscillations (both behaviors have been observed experimentally [12]). Their model suggested that other G-CSF treatment schemes (such as administering G-CSF every other day) could be effective while using less G-CSF. However, this model included neither erythrocyte nor platelet dynamics even though clinical data indicates oscillations in those cell lines in cyclical neutropenia patients. Thus it is not known if the results would be consistent with observed platelet and reticulocyte data. Second, the simulations did not take into account the pharmacokinetics of G-CSF.

Materials and methods

Data

We use data on seven grey collies generously supplied by Dr. David C. Dale (University of Washington School of Medicine, Seattle, WA, USA) and previously analyzed in Haurie et al. [7]. All of these dogs showed statistically significant cycling in neutrophils and/or platelets, according to the Lomb periodogram analysis carried out in Haurie et al. [7]. Data for neutrophils, erythrocytes, and platelets were available for untreated dogs as well as dogs receiving daily G-CSF.

Model development

The model we have developed includes the hematopoietic stem cells, the neutrophils, platelets, and erythrocytes, as well as tissue G-CSF levels and circulating G-CSF in the blood. It therefore has

four distinct cellular compartments and two compartments representing G-CSF (Fig. 1).

The stem cells are pluripotent and self-renewing, and can differentiate into the neutrophil, erythrocyte, or platelet lineages. Alternatively, the stem cells may reenter the proliferative phase of the stem cell compartment, during which they undergo a random loss via apoptosis at rate γ_S . The stem cell compartment model is based on the original work of Mackey [21]. The neutrophil, erythrocyte, and platelet compartments are modeled after earlier efforts [11,22–24]. G-CSF, meanwhile, is injected into the tissue compartment and enters the circulation from there. It is cleared from the circulation by two processes: a random loss, and a linear neutrophil-mediated clearance representing the fact that neutrophils take up circulating G-CSF [25,26]; at very high G-CSF levels the neutrophil-mediated clearance is saturable, but at the concentrations relevant here, a linear approximation is accurate.

Our notation is as follows. The hematopoietic stem cells are denoted by Q (in units of 10^6 cells/kg, see Fig. 1). The circulating neutrophils, erythrocytes, and platelets are denoted N (units 10^8 cells/kg), R (units 10^{11} cells/kg), and P (units 10^{10} cells/kg), respectively. Each of the differentiation rates from the stem cell compartment into the cell lineages depend on the number of circulating mature cells of the relevant type. These are negative feedback functions, so when the number of circulating mature cells of a given type decreases, the corresponding differentiation rate increases to compensate. The rates of differentiation (units of days^{-1}) from the HSCs into the three lineages are denoted by $\kappa_N(N)$, $\kappa_R(R)$, and $\kappa_P(P)$, respectively. Tissue levels of G-CSF are denoted X (units $\mu\text{g}/\text{kg}$), and circulating G-CSF concentration is G (units $\mu\text{g}/\text{mL}$).

The effects of G-CSF on the system (injected with a temporal schedule $I(t)$) are ultimately represented by changes in three

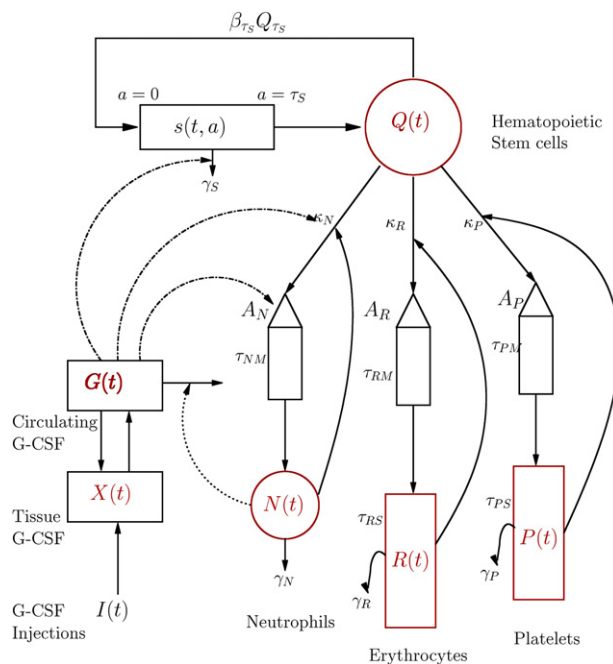


Figure 1. Schematic diagram of the model. Solid lines reflect either the movement of cells or the influence of a cell population on a process, while dashed lines represent the coupling between the G-CSF dynamics and the hematological model. The notation $Q_{\tau_S} \equiv Q(t - \tau_S)$ indicates that there is a delay involved.

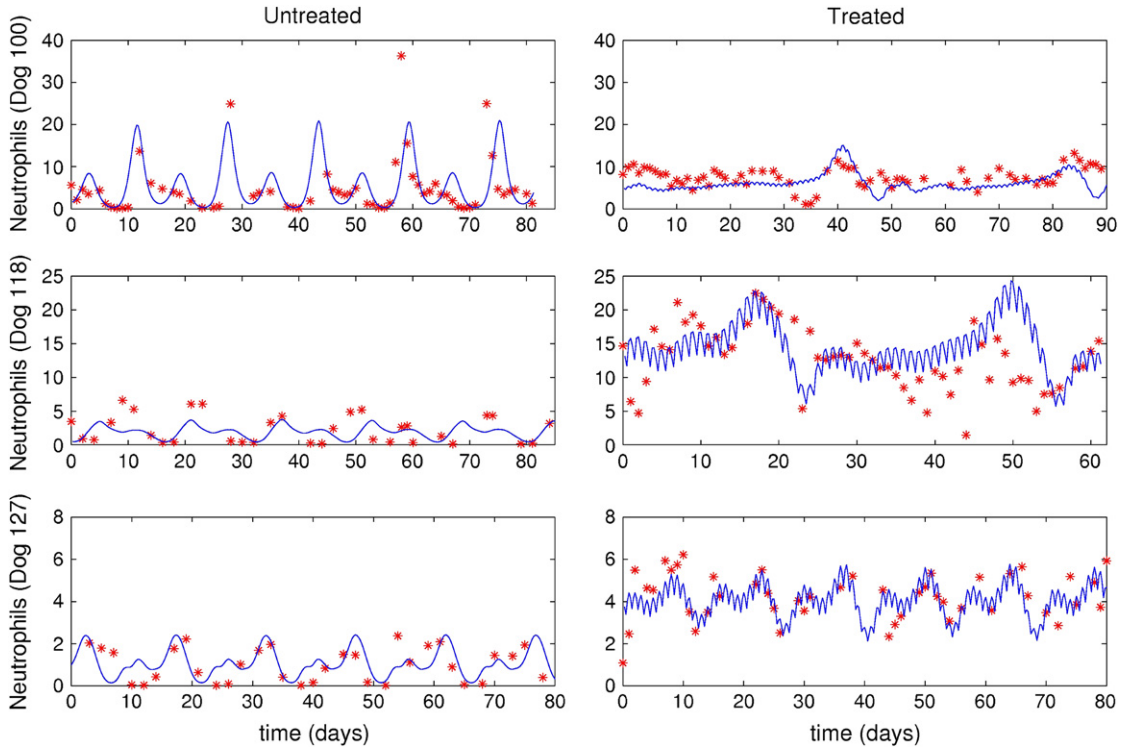


Figure 2. Serial neutrophil data and simulations for dogs 100, 118, and 127 (data and simulations for platelets and erythrocytes are not shown). The left panel shows untreated data (points) and simulations (solid line). The right panel shows data and simulations for dogs under daily G-CSF treatment. Note that the model accounts for the different scalings in neutrophil counts. The simulations were obtained using parameters resulting from the simulated annealing method. Neutrophil units are 10^8 cells-kg $^{-1}$.

parameters: A_N , the effective amplification in the neutrophil line between the HSCs and the circulating neutrophils; γ_S , the rate of apoptosis in the HSC compartment and θ_1 , through which G-CSF increases the level of differentiation from the stem cells into the neutrophil line. Only the circulating, and not the tissue, G-CSF has these effects. These particular effects are isolated because in Colijn and Mackey [1], these were the primary parameter changes that were found necessary for model simulations to match the observed laboratory and clinical data for dogs and humans with cyclical neutropenia undergoing G-CSF treatment. Furthermore, it was consistently necessary to change all three of these parameters to mimic data. With this notation, and the convention that $X_\tau \equiv X(t - \tau)$, the model equations are given by:

$$\begin{aligned} \frac{dQ}{dt} &= -\beta(Q)Q - (\kappa_N + \kappa_R + \kappa_P)Q + 2e^{-\gamma_S(G)\tau_S} \beta(Q_{\tau_S})Q_{\tau_S} \\ \frac{dN}{dt} &= -\gamma_N N + A_N(G)\kappa_N(N_{\tau_N})Q_{\tau_N} \\ \frac{dR}{dt} &= -\gamma_R R + A_R \left\{ \kappa_R(R_{\tau_{RM}})Q_{\tau_{RM}} \right. \\ &\quad \left. - e^{-\gamma_R\tau_{RS}} \kappa_R(R_{\tau_{RM}+\tau_{RS}})Q_{\tau_{RM}+\tau_{RS}} \right\} \\ \frac{dP}{dt} &= -\gamma_P P + A_P \left\{ \kappa_P(P_{\tau_{PM}})Q_{\tau_{PM}} \right. \\ &\quad \left. - e^{-\gamma_P\tau_{PS}} \kappa_P(P_{\tau_{PM}+\tau_{PS}})Q_{\tau_{PM}+\tau_{PS}} \right\} \\ \frac{dX}{dt} &= I(t) + k_T V_B G - k_B X \end{aligned}$$

$$\frac{dG}{dt} = \frac{k_B}{V_B} X - k_T G - (\alpha N + \gamma_G) G.$$

Details of the negative feedback functions, the functions $A_N(G)$ and $\gamma_S(G)$, and the G-CSF input $I(t)$ are discussed in the Appendix along with the estimation of the constant parameters.

Parameter estimation

Here, we need to find parameters that match simulations from the model containing G-CSF to observed data for each dog both during and without treatment. We begin with the fits from [1] for 7 dogs without G-CSF treatment. These were found for the model without explicit inclusion of G-CSF, and various parameters were modified in that earlier work to mimic treatment. The fits from [1] to untreated data provide our values A_N^{untr} , γ_S^{untr} , and θ_1^{untr} for each dog (see Eq. (5) in the Appendix).

For three dogs, we then use an automated, simulated annealing procedure to minimize the least squares difference between the simulation and the treated data, changing only A_N , γ_S , and θ_1 from the untreated values, and using the model without explicit G-CSF. The results are values A_N^{tr} , γ_S^{tr} , and θ_1^{tr} for these three dogs. We then estimate, without fitting, the treated parameters for the remaining 4 dogs. Table 1 lists the parameters of the model.

Treatment schedules

Having determined both the untreated and treated parameter values, we are in a position to use simulation to explore the effects of different treatment strategies. We experiment with simulating treatment every day, every second day, and every three days, for

Table 1. Normal steady state parameters appropriate for dogs

Parameter Name	Value Used	Unit	Sources
Stem Cell Compartment			
Q_*	1.1	$\times 10^6$ cells/kg	Bernard et al. [11]
γ_S	0.07	days ⁻¹	Bernard et al. [11]
τ_S	2.8	days	Bernard et al. [11], Abkowitz et al. [31]
k_0	8.0	days ⁻¹	Bernard et al. [11]
θ_2	0.5	$\times 10^6$	Bernard et al. [11]
s	4	(none)	Bernard et al. [11]
Neutrophil Compartment			
N_*	6.9	$\times 10^9$ cells/kg	Abkowitz et al. [31], Beutler et al. [32]
γ_N	2.4	days ⁻¹	Bernard et al. [11], Deubelbeiss et al. [33], Haurie et al. [34]
τ_{MN}	3.5	days	Bernard et al. [11]
A_N	752	100's	Colijn and Mackey [1]
f_0	0.40	days ⁻¹	(calculated)
θ_1	0.36	$\times 10^8$ cells/kg	Bernard et al. [11]
n	1	(none)	Bernard et al. [11]
Erythrocyte Compartment			
R_*	3.5	$\times 10^{11}$ cells/kg	Mahaffy et al. [35]
γ_R	0.001	days ⁻¹	Mahaffy et al. [35]
τ_{RM}	6	days	Mahaffy et al. [35]
τ_{sum}	120	days	Mahaffy et al. [35]
τ_{ret}	2.8	days	Beutler et al. [32]
A_R	5.63	10,000's	Beutler et al. [32], Novak and Necas [36]
\bar{k}_r	0.5	days ⁻¹	(calculated)
K_r	0.0382	$(\times 10^{11} \text{ cells/kg})^{-1}$	Mahaffy et al. [35]
m_e	6.96	(none)	Mahaffy et al. [35]
Platelet Compartment			
P_*	2.14	$\times 10^{10}$ cells/kg	Santillan et al. [22]
γ_P	0.15	days ⁻¹	Santillan et al. [22]
τ_{PM}	7	days	Santillan et al. [22]
τ_{PS}	9.5	days	Santillan et al. [22]
A_P	28.2	1000's	Beutler et al. [32]
\bar{k}_p	1.17	days ⁻¹	(calculated)
K_p	11.66	$(\times 10^{10} \text{ cells/kg})^{-1}$	Santillan et al. [22]
r	1.29	(none)	Santillan et al. [22]
G-CSF compartment			
X_*	0.1	$\mu\text{g}/\text{kg}$	(calculated)
G_*	0	$\mu\text{g}/\text{ml}$	(calculated)
k_T	0.07	hours ⁻¹	Hayashi et al. [27]
k_B	0.25	hours ⁻¹	fit
V_B	76	mL/kg	Hayashi et al. [27]
α	0.03	kg/hr	Stute et al. [25], Kearns et al. [30], fit
γ	0.07	hours ⁻¹	Vainstein et al. [29], fit
a	2.2	$\mu\text{g} * \text{hours}/\text{kg}$	(calculated)
σ^2	0.001	hours ²	(calculated)
T	24	hours	(calculated)
\bar{G}	0.01	$\mu\text{g}/\text{ml}$	(calculated)
m	1	(none)	(calculated)

each of the dogs. We also examine the effect of changing the time in the cycle when treatment is first initiated.

Results

Parameter estimation

Upon adding the G-CSF compartment and using parameters estimated from the model without it, we find that the qual-

ity of the fits to observed data is preserved. In other words, the least squares difference between the model and simulations is as good, or better, with the G-CSF compartment than without (i.e., in [1]), though the parameters were estimated for the model without it.

Figure 2 shows the fit of the untreated and treated data for dogs 100, 118, and 127, for which parameters were found with the automated simulated annealing method.

Table 2. Parameters used for computation for each dog. The other parameters are the same as in Table 1

Parameter Name	Dog 100	Dog 118	Dog 127	Dog 101	Dog 113	Dog 117	Dog 128
A_N^{untr}	488	73.4	18.8	135.8	51	659	100
A_N^{tr}	912.4	866.4	68.3	900	200	2000	800
θ_1^{untr}	0.36	0.36	0.36	0.36	0.36	0.36	0.8
θ_1^{tr}	2.0	4.1	2.1	4	4	4	5
γ_S^{untr}	0.03	0.03	0.005	0.05	0.01	0.05	0.08
γ_S^{tr}	0.17	0.15	0.05	0.18	0.055	0.1	0.18
τ_S	2.80	2.80	2.80	2.52	2.45	2.52	2.52
k_0	1.45	1.21	1.34	1.03	1.5	1.59	1.90
f_0	0.30	0.69	1.44	0.81	0.48	0.17	0.5
A_R	5.63	5.63	5.63	5.80	5.63	5.80	5.63
τ_{PM}	7	7	7	6.9	5.27	6.9	7
A_P	21.63	49.38	30.88	91.74	6.15	14.0	21.0
\bar{k}_P	1.38	1.16	0.26	0.32	3.48	0.69	0.90
K_P	3.41	10.82	2.46	8.01	11.66	3.79	4.0
\bar{G}	0.008	0.0038	0.0083	0.008	0.01	0.008	0.005

The corresponding parameter sets are given in the first three columns of Table 2 in the Appendix. In each case, we found that in order to match observed data, it was necessary to increase the neutrophil amplification A_N ; this corresponds to a decrease in apoptosis among neutrophil precursors. The amount of differentiation into the neutrophil line (θ_1) also needed to be substantially increased to mimic G-CSF treatment. It was also necessary to increase γ_S , the rate of stem

cell apoptosis. There is some redundancy in the model, in that increasing the neutrophil amplification and the differentiation into the neutrophil line from the stem cells have similar effects. This is not unexpected, since the primary effect of both changes is to raise neutrophil levels.

We estimate similar parameter changes for the remaining dogs: 101, 113, 117, and 128 (see the four last columns in Table 2 of the Appendix), and find that the simulations

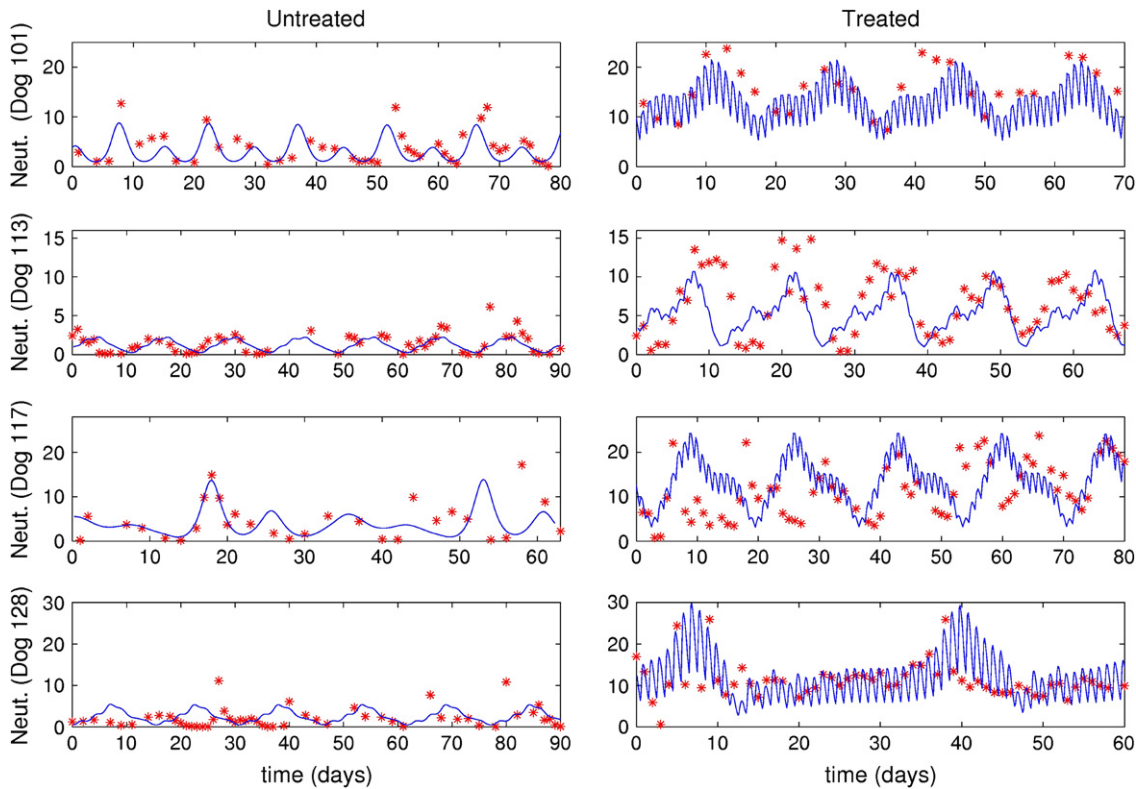


Figure 3. Serial neutrophil data and simulation results for dogs 101, 113, 117, and 128. The left panel shows data from untreated dogs (points) and simulations (solid line). The right panel shows data and simulations for dogs given daily G-CSF treatment. Note that the model accounts for the different scalings in neutrophil counts. The simulations were carried out using parameters estimated from the data from dogs 100, 118, and 127. Neutrophil units are 10^8 cells-kg⁻¹.

match the data reasonably well for the neutrophils (Fig. 3) as well as for the erythrocytes and platelets (not shown). This confirms that the new model, with the G-CSF coupled to the cell population dynamics, is capable of reproducing the data. The least-squares differences between the simulations and the data were not significantly less than the values reported in Colijn and Mackey [1]. These were the estimated, not fitted, values for the treated parameters; we are able to match observed data without automated parameter fitting based simply on an examination of the treated data and the parameter changes for dogs 100, 118, and 127.

Treatment schedules

For each dog, we perform simulations comparing daily treatment, treatment every other day, and treatment every three days. We find that particularly for dogs 100, 101, 118, and 127, changing the period of the treatment can significantly affect the nature of the oscillations. Figure 4 shows the results of treating dog 118 every other day, rather than every day.

We also explore the effects of changing the time at which the treatment is initiated. In most cases, this does not significantly change the long-term behavior. However, for dog 127 the amplitude of the oscillations is significantly

reduced when the treatment is initiated in the latter half of the cycle. More specifically, measured from day 1 (defined here to be the day when the neutrophil level reaches its minimum), we find that smaller oscillations occur if treatment is initiated on day 8 or afterwards, or on days 2 or 5 (see Fig. 5). When treatment is initiated on other days, larger oscillations in the model results. We were aware from our previous study [20] of similar models that there is the possibility that two or more qualitatively different states can be locally stable, and we have also found evidence for this in the present model. Namely, changing the treatment onset time from day 1 to day 8 for dog 127 caused the simulation to stabilize to two very different types of behavior.

It should also be noted that increasing the G-CSF dosage in the model sometimes helped to stabilize oscillations (dog 127), but in several cases (dogs 100, 128, and 101) a dosage increase from 5 $\mu\text{g}/\text{kg}$ to a dosage in the range of 15 to 25 $\mu\text{g}/\text{kg}$ caused some simulations to fail. In those simulations, the differentiation rate out of the stem cells was so high, and the apoptosis rate in the stem cells was so high, that the stem cell population was no longer able to maintain itself. For the other dogs, there was always a dosage that was sufficiently high to terminate the simulation, but it was sometimes a factor of 10 higher than the actual dosage given.

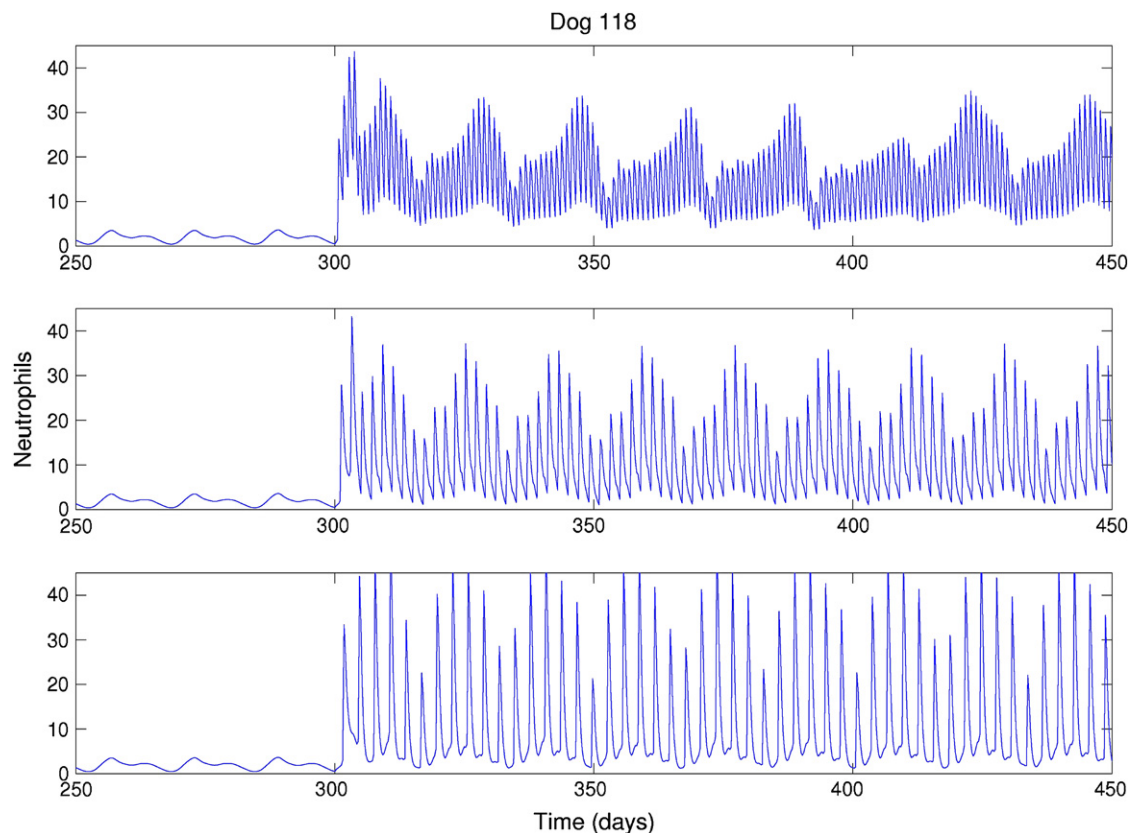


Figure 4. Simulations for dog 118 when we administer G-CSF daily (top panel), every other day (middle panel), and every third day (bottom panel). Treatment always starts on day 300. Notice the change in the amplitude of the oscillations depending on the treatment regime. Neutrophil units are in $10^8 \text{ cells}\cdot\text{kg}^{-1}$.

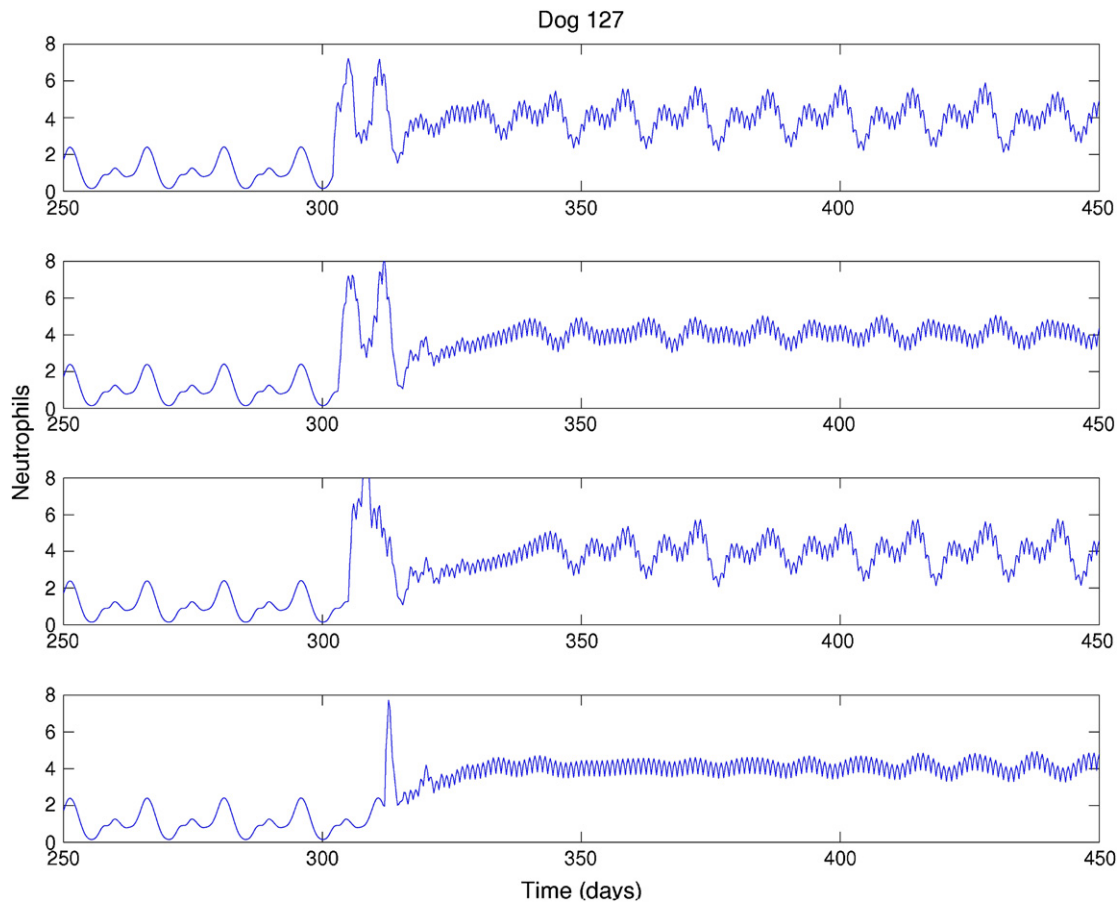


Figure 5. Simulations for dog 127 when we change the time at which daily G-CSF treatment is initiated. If day 1 represents the day at which the nadir occurs, we see starting treatment day (STD) is 1 (top), STD = 2 (second panel), STD = 4 (third panel), and STD = 9 (bottom). We can either have large amplitude oscillations (panels 1 and 3) or small oscillations (panels 2 and 4). Neutrophils are in units of 10^8 cells-kg⁻¹.

Conclusion

We have developed a model of the hematopoietic system (including the bone marrow stem cells, circulating neutrophils, platelets, and erythrocytes) that includes a pharmacokinetic model of G-CSF dynamics in tissue and in circulation. The model is able to account for the features of untreated and G-CSF-treated data for dogs with cyclical neutropenia. This is accomplished by fitting parameters for 3 dogs and thereby estimating, not fitting, parameters for 4 other dogs.

One of the most intriguing observations resulting from the parameter fitting in this study, as in Colijn and Mackey [1], is that to fit observed data for cyclical neutropenic dogs and human patients during G-CSF treatment it was necessary to model an increase in the rate of apoptosis γ_S in the stem cell compartment during G-CSF treatment. Decreasing the rate of reentry k_0 into the proliferative phase of the stem cells, which would mimic terminal differentiation that bypasses cell division in the HSC compartment, does not have the same dynamical effect on oscillations that increasing γ_S does. However, we are aware that an examination of the impact of G-CSF on HSC models would

require a more detailed investigation of the proliferation/maturation process. It was also necessary to model the more expected increase in neutrophil amplification (consistent with an inhibition of apoptosis in the proliferating neutrophil precursors).

Our results indicate that changing the period of the treatment from daily to every other day, and then to every third day, almost always significantly alters the nature of the oscillations. Furthermore, we found in one case (dog 127) that changing the time of onset of treatment to the latter half of the cycle (as measured by setting day 1 to be the day when the neutrophil level is minimal) results in much smaller amplitude oscillations in the treated simulation. Since G-CSF is costly and may have painful side effects, it may be worth exploring this option further in humans. Preliminary investigations with this model indicate that for humans, the same qualitative conclusion holds, namely that different timing and schedules have significant impact on the oscillations. However, in humans it is often impractical to collect the daily (or, even more useful for modeling purposes, more frequent than daily) cell counts that would be needed to inform modeling efforts.

In the model, both of these interventions (changing the treatment period, and changing the onset time) had more significant effects on the oscillations than did changing the G-CSF dosage. Indeed, increasing the dosage was not seen to be a viable option in our simulations, as it frequently led to the termination of the simulation rather than to the stabilization of oscillations.

The observed data are highly variable from one dog to another, but the simulations can be individualized to account for this. This presents the possibility of using “real-time” data for a given dog to individualize model simulations and make predictions about the effects of different treatment schedules.

Earlier modeling work also suggested that significantly different behavior would result from different G-CSF treatment schedules [20]. Our model substantiates this, and quantifies the effects using realistic G-CSF dynamics and yielding simulations that are directly comparable to observed data. Our central result is that in the model, changing the time of treatment initiation and/or the period of treatment may result in equally good, or better, long-term outcomes and may require less G-CSF. These changes would be practical to implement and, if less G-CSF were required, would reduce the risk of side effects as well as the cost of treatment.

Acknowledgments

This work was supported by the Natural Sciences and Engineering Research Council (NSERC grant OGP-0036920, Canada) and MITACS. We thank Prof. David C. Dale of the University of Washington for generously sharing the grey collie data with us.

Appendix: The model

Model structure

The model has several negative feedback functions that regulate stem cell proliferation and differentiation into the three circulating cell types. In this model, as in the one presented in [1], these are given by:

$$\begin{aligned} \beta(Q) &= k_0 \frac{\theta_2^s}{\theta_2^s + Q^s} \\ \kappa_N(N) &= f_0 \frac{\theta_1^n}{\theta_1^n + N^n} \\ \kappa_P(P) &= \frac{\bar{\kappa}_p}{1 + K_p P^\tau} \\ \kappa_R(R) &= \frac{\bar{\kappa}_r}{1 + K_r R^{m_e}} \end{aligned}$$

We must also specify an input function I(t) that represents the subcutaneous G-CSF injections. We assume that this in-

put is brief in duration, and that the total amount of G-CSF added corresponds to the desired dosage, namely:

$$\int_{\text{before}}^{\text{after}} I(t) dt = \text{dosage}.$$

Note that if σ is small, a Gaussian-like input approximates a Dirac δ -function, and we can write

$$\int_{\text{before}}^{\text{after}} a e^{-t^2/\sigma^2} dt \approx \int_{-\infty}^{\infty} a e^{-t^2/\sigma^2} dt = a\sigma\sqrt{\pi}.$$

Therefore to simulate periodic injections, we let

$$I(t) = H(t - d) a e^{-((t \bmod T) - T/2)^2/\sigma^2},$$

where H (t) denotes the Heaviside step function

$$H(t) = \begin{cases} 0 & t \leq 0 \\ 1 & t > 0. \end{cases}$$

The day on which treatment is initiated is denoted by d, and the Heaviside function simply turns the injections on. The term “t mod T” ensures periodicity, and we require that $T \gg \sigma$ so that the approximation to the integral remains valid. Finally, we ensure that (3) holds by choosing the parameter a such that $a\sigma\sqrt{\pi} = \text{dosage}$. It remains only to describe how the G-CSF acts on the hematological portion of the model. Because we believe from previous modeling efforts that A_N , γ_S , and θ_1 are the parameters that need to change under G-CSF, we model G-CSF injections as causing fluctuations in these three parameters:

$$\begin{aligned} A_N &= A_N^{\text{untr}}(1 - H(t - d)) + H(t - d)(m_A(G - \bar{G}) + A_N^{\text{tr}}) \\ \gamma_S &= \gamma_S^{\text{untr}}(1 - H(t - d)) + H(t - d)(m_g(G - \bar{G}) + \gamma_S^{\text{tr}}) \\ \theta_1 &= \theta_1^{\text{untr}}(1 - H(t - d)) + H(t - d)(m_r(G - \bar{G}) + \theta_1^{\text{tr}}) \end{aligned}$$

The superscripts “tr” and “untr” respectively indicate values corresponding to values that, in the model without the dynamics of G-CSF, match treated and untreated data respectively. The parameters m_A , m_g , and m_r are slopes that specify how much A_N , γ_S , and θ_1 change in response to a given change in G-CSF concentration, G. \bar{G} is the average G-CSF concentration for each data set. These were computed using the G-CSF model alone (without the cell types coupled to it), and using the average neutrophil levels in each data set.

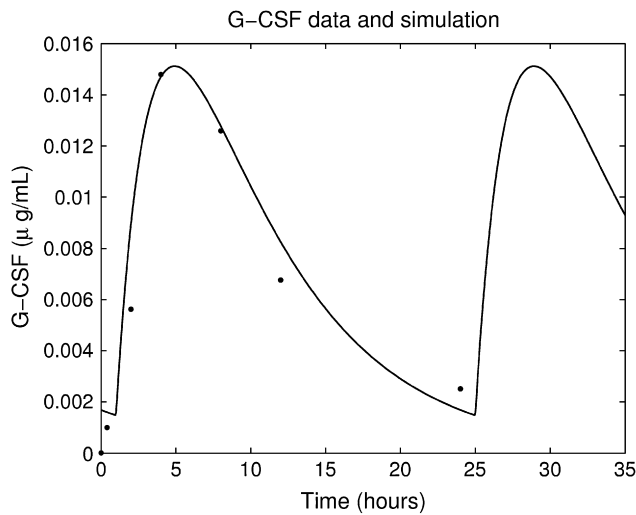


Figure 6. Predicted serum G-CSF time series compared to digitized data from Stute et al. [25].

The slopes were computed as follows:

$$\begin{aligned} m_A &= m(A_N^{\text{tr}} - A_N^{\text{untr}}) / \bar{G} \\ m_g &= m(\gamma_S^{\text{tr}} - \gamma_S^{\text{untr}}) / \bar{G} \\ m_t &= m(\theta_1^{\text{tr}} - \theta_1^{\text{untr}}) / \bar{G}. \end{aligned}$$

In (5), m_A , m_g , and m_t set the amount of fluctuation in A_N , γ_S , and θ_1 . When the parameter m in (6) is 1, then when G falls to zero, A_N , γ_S , and θ_1 drop all the way down to their average untreated levels. If $m < 1$, then they do not fall all the way to their untreated average levels when $G = 0$ but rather fluctuate about their treated levels with a lower amplitude. (This can be seen by rearranging (5) and (6), setting $t > d$ to get $A_N - A_N^{\text{tr}} = m(A_N^{\text{tr}} - A_N^{\text{untr}})(\bar{G}/G)$.)

Parameter estimation

There are a number of parameters to be estimated, and many of these have been considered in previous modeling studies [1,2,11]. Our baseline parameters for the HSC compartment, and the neutrophil, platelet, and erythrocyte compartments, are the same as in Colijn and Mackey [1]. Colijn and Mackey [1,2] can be consulted for an extensive discussion of how these parameters were determined.

Some of the pharmacokinetic parameters for the G-CSF portion of the model can be taken from published data on G-CSF kinetics. We require estimates of the transfer rates k_T and k_B , the volume V_B , and the parameters α and γ_G , which give the clearance rate of G-CSF from the bloodstream. Hayashi et al. [27] and Kuwabara et al. [28] determined $k_T = 0.06 \text{ hr}^{-1}$ and $V_B = 76 \text{ mL/kg}$, while Vainstein et al. [29] give $\gamma = 0.06 \text{ hr}^{-1}$. We use $k_B = 0.25 \text{ hr}^{-1}$, which is larger than the value 0.1 given in Hayashi et al.

[27] but which we needed to reach the observed levels of G-CSF using the approximate $I(t)$ input. It only remains to estimate α , which relates the number of circulating neutrophils to the clearance of G-CSF. Given a known value for N on the day of treatment, and the G-CSF concentration as a function of time, the half-life can be related to the clearance rate by $t_{1/2} = \ln 2 / (\alpha N + \gamma)$. With the half-lives and circulating neutrophil counts in Stute et al. [25] and Kearns et al. [30], this gives a range of α between 0.015 and 0.03 kg/hr. To check the validity of this determination, and to ensure that the model is giving a reasonable description of G-CSF dynamics, we digitized a time series of G-CSF concentration from Stute et al. [25] and fit the model simulations to these data. The fit is shown in Figure 6. The value of α from the fit is 0.03, consistent with the above estimate.

References

- Colijn C, Mackey M. A mathematical model of hematopoiesis: II. Cyclical neutropenia. *J Theor Biol.* 2005;237:133–146.
- Colijn C, Mackey M. A mathematical model of hematopoiesis: I. Periodic chronic myelogenous leukemia. *J Theor Biol.* 2005;237:117–132.
- Haurie C, Mackey MC, Dale DC. Cyclical neutropenia and other periodic hematological diseases: A review of mechanisms and mathematical models. *Blood.* 1998;92:2629–2640.
- Guerry D, Dale D, Omine DC, Perry S, Wolff SM. Periodic hematopoiesis in human cyclic neutropenia. *J Clin Invest.* 1973;52:3220–3230.
- Dale DC, Hammond WP. Cyclic neutropenia: A clinical review. *Blood Rev.* 1988;2:178–185.
- Haurie C, Dale DC, Rudnicki R, Mackey MC. Modeling complex neutrophil dynamics in the grey collie. *J Theor Biol.* 2000;204:505–519.
- Haurie C, Person R, Dale DC, Mackey M. Haematopoietic dynamics in grey collies. *Exp Hematol.* 1999;27:1139–1148.
- Horwitz M, Benson K, Person R, Aprikyan A, Dale D. Mutations in *ela2*, encoding neutrophil elastase, define a 21-day biological clock in cyclic haematopoiesis. 1999;23:433–436.
- King-Smith EA, Morley A. Computer simulation of granulopoiesis: Normal and impaired granulopoiesis. *Blood.* 1970;36:254–262.
- Morley A, King-Smith EA, Stohlman F. The oscillatory nature of hemopoiesis. In: Stohlman F, ed. Hemopoietic Cellular Proliferation. New York: Grune & Stratton; 1969. p. 3–14.
- Bernard S, Bélair J, Mackey M. Oscillations in cyclical neutropenia: New evidence based on mathematical modeling. *J Theor Biol.* 2003; 223:283–298.
- Hammond WP, Price TH, Souza LM, Dale DC. Treatment of cyclic neutropenia with granulocyte colony stimulating factor. *N Engl J Med.* 1989;320:1306–1311.
- Koury M. Programmed cell death (apoptosis) in hematopoiesis. *Exp Hematol.* 1992;20:391–394.
- Park JR. Cytokine regulation of apoptosis in hematopoietic precursor cells. *Curr Opin Hematol.* 1996;3:191–196.
- Migliaccio AR, Migliaccio G, Dale DC, Hammond WP. Hematopoietic progenitors in cyclic neutropenia: Effect of granulocyte colony stimulating factor in vivo. *Blood.* 1990;75:1951–1959.
- Williams G, Smith C. Molecular regulation of apoptosis: Genetic controls on cell death. *Cell.* 1993;74:777–779.
- Ozer H, Armitage JO, Bennett CL, et al. Update of recommendations for the use of hematopoietic colony-stimulating factors: Evidence-based, clinical practice guidelines. *J Clin Oncol.* 1997;10:3288.

18. Dale DC, Cottle TE, Fier CJ. Severe chronic neutropenia: Treatment and follow-up of patients in the severe chronic neutropenia international registry. *Am J Hematol.* 2003;72:82–93.
19. Jayabose S, Sandoval C. Recombinant human granulocyte colony stimulating factor in cyclic neutropenia: Use of a new 3-day-a-week regimen. *Am J Pediatr Hematol Oncol.* 1994;16:338–340.
20. Foley C, Bernard S, Mackey M. Cost-effective G-CSF therapy strategies for cyclical neutropenia: Mathematical modelling based hypotheses. *J Theor Biol.* 2006;238:754–763.
21. Mackey MC. A unified hypothesis for the origin of aplastic anemia and periodic haematopoiesis. *Blood.* 1978;51:941–956.
22. Santillan M, Mahaffy J, Bélair J, Mackey M. Regulation of platelet production: The normal response to perturbation and cyclical platelet disease. *J Theor Biol.* 2000;206:585–603.
23. Bélair J, Mackey M, Mahaffy J. Age-structured and two-delay models for erythropoiesis. *Math Biosci.* 1995;128:317–346.
24. Mahaffy J, Bélair J, Mackey M. Hematopoietic model with moving boundary condition and state dependent delay: Applications in erythropoiesis. *J Theor Biol.* 1998;190:135–146.
25. Stute N, Santana V, Rodman J, Schell M, Ihle J, Evans W. Pharmacokinetics of subcutaneous recombinant human granulocyte colony-stimulating factor in children. *Blood.* 1992;79:2849–2854.
26. Takatani H, Soda H, Fukuda M, et al. Levels of recombinant human granulocyte colony stimulating factor in serum are inversely correlated with circulating neutrophil counts. *Antimicrob Agents Chemother.* 1996;40:988–991.
27. Hayashi N, Aso H, Higashida M, et al. Estimation of rhg-csf absorption kinetics after subcutaneous administration using a modified Wagner-Nelson method with a nonlinear elimination model. *Eur J Pharm Sci.* 2001;15:151–158.
28. Kuwabara T, Kato Y, Kobayashi S, Suzuki H, Sugiyama Y. Nonlinear pharmacokinetics of a recombinant human granulocyte colony-stimulating factor derivative (nartograstim): Species differences among rats, monkeys and humans. *J Pharmacol Exp Ther.* 1994;271:1535–1543.
29. Vainstein V, Ginosara Y, Shohamb M, Ranmara D, Ianovskib A, Agur Z. The complex effect of granulocyte colony-stimulating factor on human granulopoiesis analyzed by a new physiologically-based mathematical model. *J Theor Biol.* 2005;234:311–327.
30. Kearns CM, Wang WC, Stute N, Ihle J, Evans WE. Disposition of recombinant human granulocyte colony-stimulating factor in children with severe chronic neutropenia. *J Pediatr.* 1993;123:471–479.
31. Abkowitz JL, Holly RD, Hammond WP. Cyclic hematopoiesis in dogs: Studies of erythroid burst forming cells confirm an early stem cell defect. *Exp Hematol.* 1988;16:941–945.
32. Beutler E, Lichtman MA, Coller BS, Kipps T. *Williams Hematology.* New York: McGraw-Hill; 1995.
33. Deubelbeiss KA, Dancy JT, Harker LA, Finch CA. Neutrophil kinetics in the dog. *J Clin Invest.* 1975;55:833–839.
34. Haurie C, Dale DC, Rudnicki R, Mackey MC. Modeling complex neutrophil dynamics in the grey collie. *J Theor Biol.* 2000;204:504–519.
35. Mahaffy JM, Bélair J, Mackey M. Hematopoietic model with moving boundary condition and state dependent delay. *J Theor Biol.* 1998;190:135–146.
36. Novak JP, Necas E. Proliferation differentiation pathways of murine haematopoiesis: correlation of lineage fluxes. *Cell Prolif.* 1994;27:597–633.